Chapter 3 in The Physical Geography of South America.
T. Veblen, K. Young and A. Orme (Eds).
Oxford University Press, 2007.

3

Atmospheric Circulation and Climatic Variability

René D. Garreaud
Patricio Aceituno

Regional variations in South America's weather and climate reflect the atmospheric circulation over the continent and adjacent oceans, involving mean climatic conditions and regular cycles, as well as their variability on timescales ranging from less than a few months to longer than a year. Rather than surveying mean climatic conditions and variability over different parts of South America, as provided by Schwerdtfeger and Landsberg (1976) and Hobbs et al. (1998), this chapter presents a physical understanding of the atmospheric phenomena and precipitation patterns that explain the continent's weather and climate.

These atmospheric phenomena are strongly affected by the topographic features and vegetation patterns over the continent, as well as by the slowly varying boundary conditions provided by the adjacent oceans. The diverse patterns of weather, climate, and climatic variability over South America, including tropical, subtropical, and midlatitude features, arise from the long meridional span of the continent, from north of the equator south to 55°S. The Andes cordillera, running continuously along the west coast of the continent, reaches elevations in excess of 4 km from the equator to about 40°S and, therefore, represents a formidable obstacle for tropospheric flow. As shown later, the Andes not only acts as a "climatic wall" with dry conditions to the west and moist conditions to the east in the subtropics (the pattern is reversed in midlatitudes), but it also fosters tropical-extratropical interactions, especially along its eastern side. The Brazilian plateau also tends to block the low-level circulation over subtropical South America. Another important feature is the large area of continental landmass at low latitudes (10°N–20°S), conducive to the development of intense convective activity that supports the world's largest rain forest in the Amazon basin. The El Niño–Southern Oscillation phenomenon, rooted in the ocean-atmosphere system of the tropical Pacific, has a direct strong influence over most of tropical and subtropical South America. Similarly, sea surface temperature anomalies over the Atlantic Ocean have a profound impact on the climate and weather along the eastern coast of the continent.

3.1 Mean Climatic Features and Regular Cycles

In this section we describe the long-term annual and monthly mean fields of several meteorological variables. These climatological fields are obtained by averaging many daily fields, each of them constructed on the basis of surface, upper-air, and satellite meteorological observations. The atmospheric circulation (winds, pressure, etc.) is characterized by using the NCEP-NCAR reanalysis from 1979 to 1995 (Kalnay et al., 1996). The precipitation fields are a blend of station data (Legates and Willmott, 1990) and precipitation estimates from the Microwave Sounding Unit (MSU) covering the period 1979 to 1992 (Spencer, 1993). While the averaging procedure does not have any physical a priori significance, the regional climate is defined by the relevant features in the mean fields, which in turn are forced by the fixed (or very slowly varying) boundary conditions of the atmosphere: land-sea distribution, continental topography, and the time/space changes of the solar radiation reaching the surface. Figure 3.1 shows the annual mean precipitation, sea-level pressure, and low-level winds [1,000–850 hecto-Pascal (hPa) average]. The maximum precipitation occurs over the tropical oceans along a band at approximately 8°N that coincides with a belt of low pressure and low-level wind convergence. This band, the so-called Intertropical Convergence Zone (ITCZ), is a major feature of the global circulation, and its year-round position to the north of the equator is ultimately related to the land-sea distribution and orientation of the coastlines (Mitchell and Wallace, 1992). The rainfall in the ITCZ decreases slightly as it straddles northern South America, in part due to the decrease in surface evaporation, but still produces the highest continental precipitation over the equatorial Andes, the western Amazon basin, and near the mouth of the Amazon River. The rainfall in this part of the continent is produced by deep, moist convection—the very energetic ascent of buoyant air from near the surface to the tropopause that sustains the largest rainforest of the world (see chapter 9).

Two other bands of high annual mean rainfall are evident in figure 3.1. The western band has its origin in the western equatorial Pacific (central Pacific during El Niño years), reaching the continent between its tip and 40°S. Precipitation in the South Pacific Convergence Zone (SPCZ; Vincent, 1998) is largely produced by extratropical frontal systems. The annual mean rainfall is high in southern Chile due to the enhanced uplift over the western slopes of the Andes (Lenters and Cook, 1995), but it decreases sharply to the east, producing rather dry conditions in Argentina's Patagonia (see also chapters 13 and 14). The eastern band has its root over the central part of the continent, and extends southeastward forming the South Atlantic Convergence Zone (SACZ; Kodoma, 1992; Figueroa et al., 1995). Rainfall over the central part of the continent is largely produced by deep convection, but as one moves into the subtropics, Southern Hemisphere (SH) frontal systems become more important in promoting deep convection and eventually produce most of the precipitation (Lenters and Cook, 1995). For instance, the uniformly large amounts of rainfall observed year round on the coast of southern Brazil and Uruguay are produced by deep con-

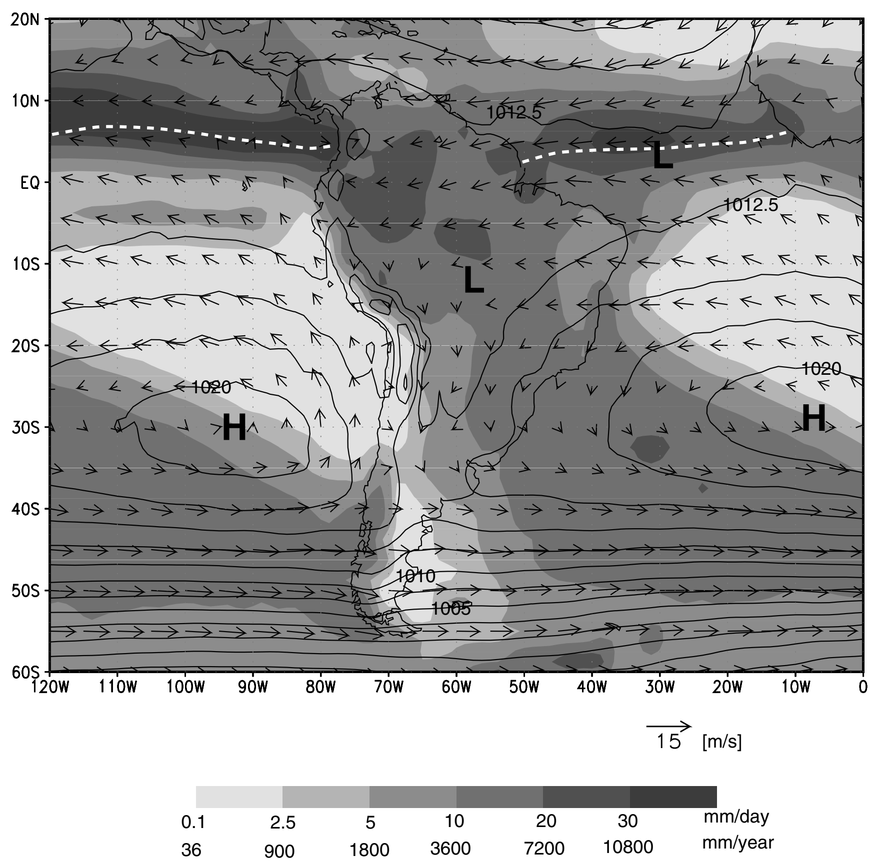

Figure 3.1 Annual mean rainfall (shading scale at bottom), sea level pressure (contoured every 2.5 hPa), and low-level winds (arrow scale at bottom). Dashed white line indicates mean position of the ITCZ. Letters H and L indicate approximate center of the subtropical anticyclones and continental low, respectively.

vection during the warm season (November to March) and by frontal systems during the cold season (Montecinos et al., 2000).

Rainfall is nearly absent over broad areas of the subtropical oceans owing to large-scale midtropospheric subsidence (fig. 3.1). The rate of subsidence is mainly dictated by the radiative cooling of the air parcels that have reached the upper troposphere over the ITCZ (Rodwell and Hoskins, 1996). The subtropical subsidence together with the ascent over the ITCZ, the low-level trade winds, and the upper-level poleward flow form the Hadley cell, a major feature of the atmosphere's general circulation. The subsiding air also maintains the very persistent cells of surface high pressure and low-level anticyclonic circulation over the southeast Pacific and Atlantic oceans, with only minor seasonal variations. Over the continent, deep convection (either moist or dry) offsets the large-scale subsidence, so that mean upward motion prevails over the central part of South America, enhancing the subsidence over the southeast Pacific Ocean (Gandu and Silva Dias, 1998).

Consequently, sea-level pressure over the continent is lower than the corresponding value over the adjacent oceans throughout the year, thus forcing the trade winds over the tropical Atlantic to penetrate into the continent in a nearly east-west direction, until they become convergent near the Andes cordillera. On the western side of the tropical-subtropical Andes (which act as an effective barrier to the flow), the equatorward low-level winds promote coastal upwelling of cold waters, maintaining a coastal tongue of low sea surface temperature (SST) that extends westward at the equator, where it is enhanced by equatorial upwelling. The adiabatically warmed air aloft and the cold SST result in a cool, moist marine boundary layer of 500–1,000 m thick capped by a strong temperature inversion over the subtropical southeast Pacific (e.g. Garreaud et al., 2002). A very extensive deck of shallow, non-precipitating stratocumulus clouds is typically observed at the top of the marine boundary layer (e.g., Klein and Hartmann, 1993). This cloud layer plays an important role in the regional and global climate by substantially reducing the amount of solar radiation reaching the ocean surface (the so-called albedo effect; e.g., Hartmann et al., 1992) and by cooling the lower troposphere due to the strong upward emission of infrared radiation at the top of the clouds (Nigam, 1997).

Two conspicuous dry regions occur over tropical-subtropical South America (fig. 3.1; see also chapter 11). The first region encompasses the western side of the continent, a 100–300 km strip of land between the coastline and the Andes cordillera from ~30°S as far north as 5°S. The coastal desert of northern Chile and Perú is primarily explained by the strong, large-scale subsidence over the subtropical southeast Pacific Ocean, but its extreme aridity (places with no precipitation for several years) seems related to regional factors (Abreu and Bannon, 1993; Rutllant et al., 2000). At these latitudes, the central Andes (including the Altiplano) become a truly climatic border between the extremely arid conditions to the west and the wet conditions to the east (e.g., Garreaud 2000a; see also chapters 10 and 12). The second region corresponds to the eastern tip of the continent, in northeast Brazil, where the annual mean precipitation is less than half of the inland values at the same latitude and the rainy season is restricted to March to May, when the ITCZ reaches its southernmost position (e.g., Kousky and Ferreira, 1981; Hastenrath, 1982). The dryness of this region appears to result from a local intensification of the Hadley cell in connection with the strong convection over the equatorial Atlantic (Moura and Shukla, 1981; Mitchell and Wallace, 1992).

The area affected by deep convection experiences significant changes during the year, leading to a pronounced mean annual cycle in rainfall over tropical and subtropical South America, as shown by seasonal maps of mean precipitation (fig. 3.2). Such changes are controlled by the annual north-south march of insolation, resulting in changes in land surface temperatures, and also by complex interactions with changes in low-level moisture transport (Fu et al., 1999). During the austral winter (June–July–August, JJA,), the heaviest precipitation and thunderstorms are found over northern South America and southern Central America, connected with the oceanic ITCZ (fig. 3.2a). At this time of year, the central part of the continent (including southern Amazonia) experiences its dry season, interrupted occasionally by the passage of modified cold fronts from the southern midlatitudes. By the end of October, there is a rapid shift of the area of intense convection from the northern extreme of the continent into the central Amazon basin (e.g., Horel et al., 1989), marking the onset of the so-called South American summer monsoon (fig. 3.2b, Zhou and Lau, 1998).

The area of convective precipitation reaches its southernmost position during the austral summer (December–January–February, DJF), encompassing the southern Amazon basin, the Altiplano, and the subtropical plains of the continent (southern Bolivia and Brazil, Uruguay, Paraguay, and central Argentina), and extending over the South Atlantic Convergence Zone (fig. 3.2c). In this season, a low pressure cell forms over the extremely hot and dry Chaco region (Seluchi and Marengo, 2000), forcing the southward flow of the trade winds and their subsequent convergence over the subtropical plains. Observational and modeling evidence has shown that the northerly flow between the Andes and the Brazilian highlands is often organized in a low-level jet with its core (wind speed often in excess of 12 m/s) at about 1 km above the ground and less than 100 km from the eastern slopes of the Andes (e.g. Saulo et al., 2000). The poleward moisture transport by this low-level jet feeds the convective rainfall over the subtropical plains, a major agricultural region and heavily populated area (Berbery and Collini, 2000; Saulo et al., 2000).

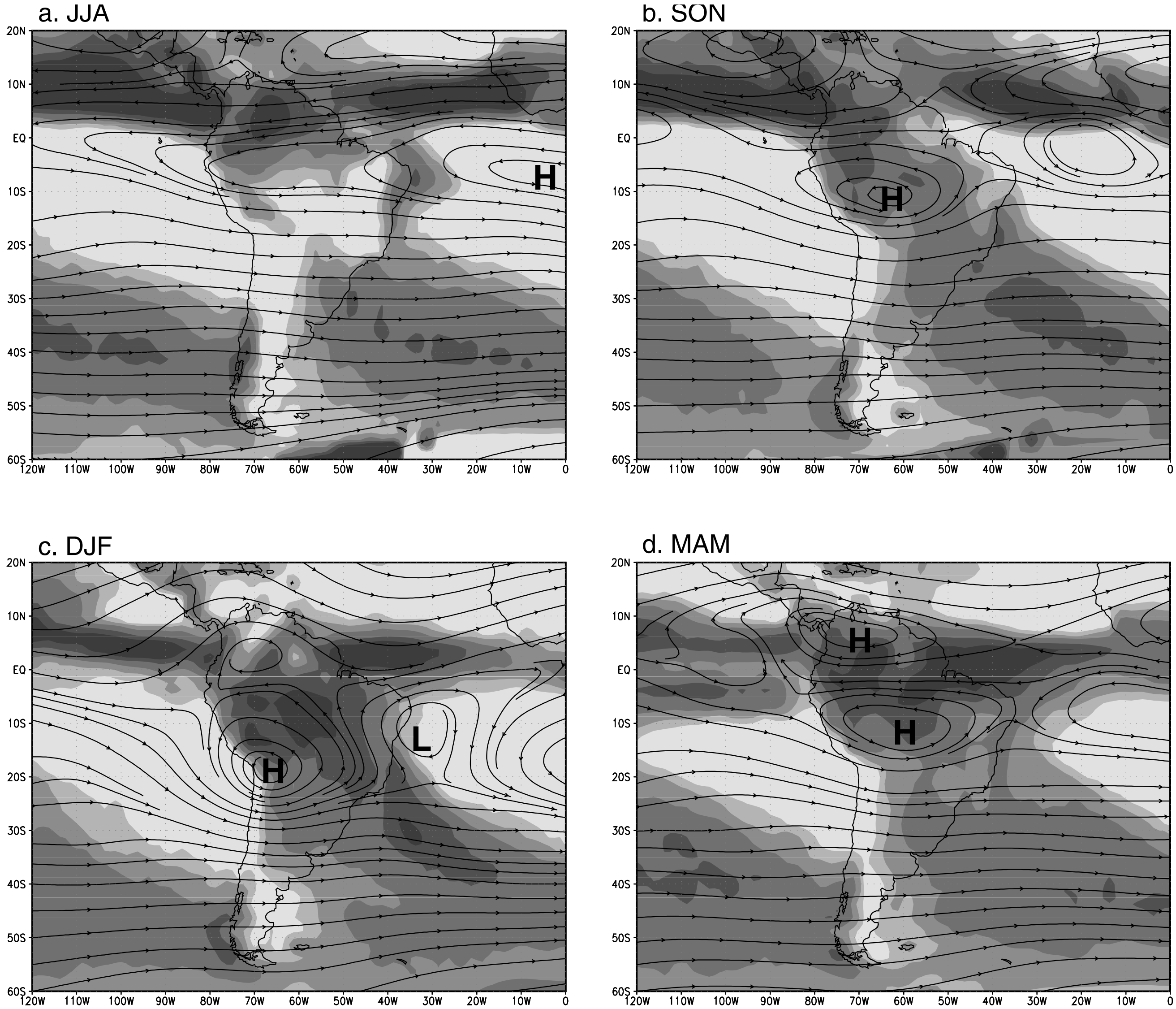

Figure 3.2 Seasonal mean rainfall (shading scale as figure 1) and 200 hPa winds (shown as streamlines) for (a) austral winter, (b) spring, (c)summer, and (d) fall. Maximum wind speed in midlatitudes is 60 m/s. Letter H indicates the approximate center of upper level anticyclones. Letter L in (c) indicates the center of the upper level trough over northeast Brazil.

During early fall, deep convection gradually diminishes over the subtropics and begins to shift northward, thus leading to the demise of the South American summer monsoon by the end of April (fig. 3.2d).

The seasonal maps in figure 3.2 show the upper-level atmospheric circulation in terms of the mean 200–hPa winds superimposed on the precipitation field. During the austral winter (JJA), strong Southern Hemisphere (SH) westerly flows prevail over South America as far north as 5°S, consistent with the equatorward displacement of the maximum tropical-extratropical thermal gradient (fig. 3.2a). During the course of the austral spring (SON), the subtropical jet stream moves southward, while a weak anticyclonic circulation develops over the tropical part of the continent (fig. 3.2b). During the austral summer (DJF), the SH westerlies over the continent are restricted to the south of 22°S, while the Northern Hemisphere (NH) westerlies reach the northern extreme of the continent. In this season, an upper-level anticyclonic circulation, referred as the Bolivian High, becomes firmly established over the central part of the continent (with its center located at 15°S and 65°W). This High is accompanied by a cyclonic circulation downstream over the northeast coast of Brazil, and a convergence region along the coast of Perú and Ecuador (fig. 3.2c; Virji 1981; Lenters and Cook, 1997).

It was originally proposed that the Bolivian High had a thermal origin, maintained by the strong sensible heating over the central Andes and the release of latent heat in the summertime convection over the Altiplano (Schwerdtfeger, 1961; Gutman and Schwerdtfeger, 1965). Modeling studies (reviewed in Lenters and Cook, 1997), however, indicate that the Bolivian High is instead a dynamical response to the warming of the upper troposphere generated by the cumulus convection over the Amazon basin. Diabatic heating over the Altiplano does not appear essential for the existence of the Bolivian High, although the Andes play an indirect role by organizing the low-level flow and convection over the central part of the continent. On the other hand, the presence of the Bolivian High is instrumental for the occurrence of summertime precipitation over the Altiplano, since the easterly flow aloft favors the transport of moist air from the lowlands toward the central Andes (Garreaud, 1999b). Furthermore, the Bolivian High contributes to the intensification of the SACZ during summer, owing to vorticity advection aloft (Figueroa et al., 1995). During the austral fall (MAM), the SH westerlies return to the subtropics, and a pair of anticyclones is found over tropical South America, consistent with the convection centered on the equator (fig. 3.2d).

During the rainy season, there is a well-known preference for an afternoon / evening maximum of deep convection over continental areas, since land-surface heating tends to destabilize the lower troposphere (e.g. Meisner and Arkin, 1987). Nevertheless, detailed analyses of the mean diurnal cycle of rainfall (Negri et al., 1994) and convective clouds (Garreaud and Wallace, 1997) demonstrate that the timing of the maximum convection is location-dependent, and closely linked to regional topographic features such as mountain ranges and concave coastlines. To illustrate this point, figure 3.3 shows the evening and early morning frequencies of cold cloudiness, a proxy for convective rainfall, during the austral summer (DJF). Maximum convection during the evening is very pronounced over the central Andes, along the northeast coast of the continent, and in two parallel bands over central Amazonia (fig. 3.3a). The first two bands arise from the concurrent timing of the thermodynamic destabilization and the maximum strength of dynamical forcing: plain-to-mountain wind convergence over the Andes, and land-sea breeze convergence along the coast. The intervening parallel bands are interpreted as the afternoon reactivation of recurrent Amazon coastal squall lines (ACSL; e.g., Cohen et al., 1995). ACSLs are forced at the coast by sea breezes and move inland, maintaining their identity for 12–36 hours, most notably in early autumn. On the other hand, convection tends to peak during night-time and early morning along the eastern slopes of the central Andes, over the subtropical plains, and off the northeast coast of the continent, highlighting the dynamical forcing in these areas (fig. 3.3b; Berbery and Collini, 2000).

The mean annual and diurnal cycles of the precipitation to the south of 40°S are generally less pronounced than those at lower latitudes, because of the dynamical forcing (in contrast with thermodynamic forcing) of frontal rainfall. A notable feature of the SH midlatitudes is the circumpolar ring of strong westerly flow throughout the depth of the troposphere; this intersects the southern tip of South America between 50°S and 40°S. As described later, the zonal symmetry observed in figure 3.2 is the result of averaging many daily maps, each of them containing significant departures from zonal symmetry and strong meridional flow. The

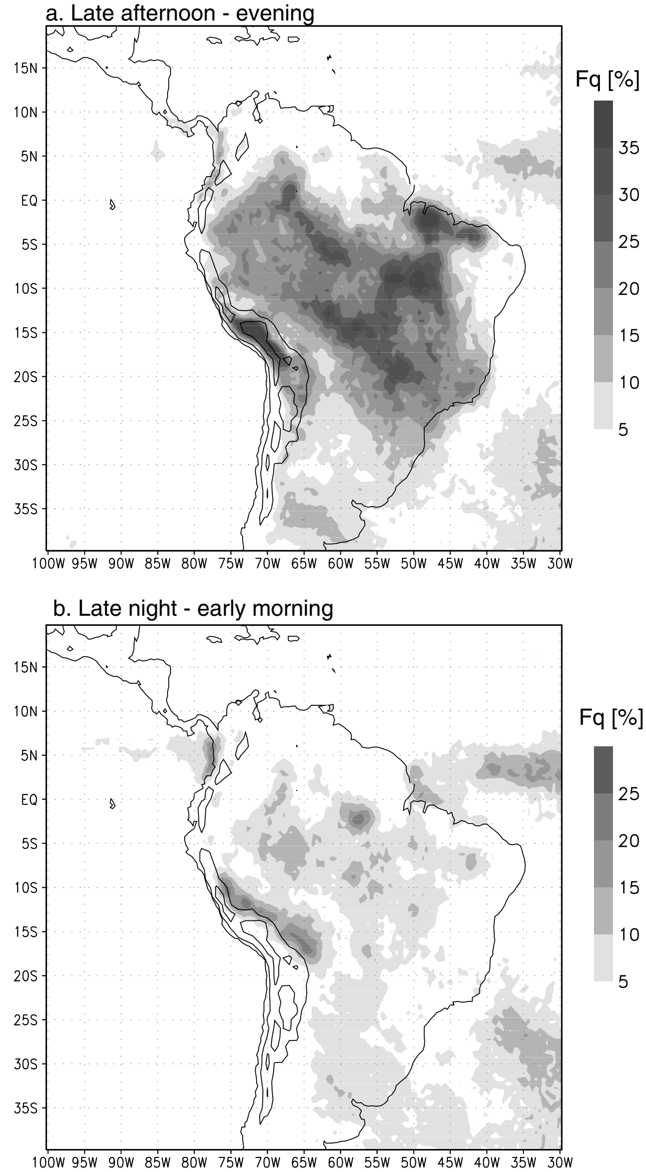

Figure 3.3 (a) Late afternoon and evening (1,800–2,100 UTC average; UTC: Universal Time Coordinated = Greenwich Time) frequency of cold clouds (cloud-top temperature less than 235°K) during the austral summer (DJF). Solid lines within the continent indicate terrain elevation at 2,000 and 4,000 m above mean sea level. (b) As (a) but for late night and early morning (0900–1,200 UTC average; modified from Garreaud and Wallace, 1997).

position of the jet axis coincides with zone of maximum meridional temperature gradient, and therefore is a proxy for the preferred path, or storm track, of synoptic-scale disturbances (Trenberth, 1991). Although subtle, there is an intensification and equatorward shift of the storm track and similar changes in the strength and position of the subtropical anticyclones during the austral winter (JJA; Physick, 1981), thus leading to the rainy season in central Chile and Argentina (30–40°S) (fig. 3.2; see also chapter 11).

3.2 High-Frequency Climatic Variability

Temporal changes in atmospheric conditions, such as temperature, rainfall, and wind, over a given region exhibit nonregular fluctuations across a broad range of scales superimposed on the mean diurnal and annual cycles. These fluctuations include synoptic-scale variability, broadly associated with weather, as well as intraseasonal, interannual, interdecadal, and longer-scale variations, that arise from the internal variability of the atmosphere and its coupling with other components of the Earth system such as the oceans, land vegetation, and sea-ice. In this section, we describe fluctuations in the atmospheric circulation and rainfall that occur on timescales ranging from a few days to a few months, usually termed high-frequency variability. These fluctuations are important in themselves because they influence weather patterns, while changes in their frequency and intensity constitute the building blocks of longer-scale variability.

3.2.1 Synoptic-Scale Variability

Synoptic variability refers to changes in atmospheric conditions over periods ranging from 2 to 10 days. These changes are caused by synoptic-scale disturbances, that is, troposphere-deep phenomena with horizontal dimensions of thousands of kilometers in at least one direction that maintain their identity for several days. The prime source of synoptic disturbances are the baroclinic waves that grow, reach maturity, and decay while embedded in the midlatitude westerly flows. Details on the dynamics, structure, and evolution of baroclinic waves can be found in most textbooks of meteorology (e.g. Wallace and Hobbs, 1977; Holton, 1992). In addition to midlatitude waves, synoptic variability can also be produced by phenomena of pure tropical origin, such as tropical depressions. Except for the influence of easterly waves along the northeast coast, these kinds of synoptic phenomena are seldom observed in South America, a fact attributed to the relatively cold sea surface temperature in the adjoining oceans (Satyamurti et al., 1998).

As mentioned earlier, the circumpolar SH storm track intersects the continent to the south of 40°S, with only minor seasonal changes. More detailed analysis by Berbery and Vera (1996) indicates the existence of two preferred west-to-east paths of baroclinic waves in the South American region: one along the subpolar jet, about 60°S, and the other along the subtropical jet that crosses the Andes between 30°S and 45°S. The baroclinic waves in the former path are little affected by continental topography, and they evolve smoothly as they move to east-southeast over the southern oceans (Vigliarolo et al., 2000). In contrast, waves evolving along the subtropical path are blocked by the Andes cordillera and experience substantial distortion in their structure. The effect of the Andes on baroclinic waves has been addressed in statistical analysis by Gan and Rao (1994b), Berbery and Vera (1996) and Seluchi et al. (1998), among others. At upper levels, the waves tend to move to the northeast, slightly departing from the general zonality. The equatorward dispersion of the wave activity is consistent with the conservation of potential vorticity of the air columns crossing the Andes cordillera (Seluchi et al., 1998). Upper level mid-latitude waves can also spawn closed cyclonic vortices (cutoff lows) that subsequently move irregularly in the subtropics, as discussed later. At lower levels, midlatitude disturbances experience major distortion due to mechanical blocking. To the west of the subtropical Andes, pressure anomalies tend to be out of phase with respect to the incoming disturbance farther south, especially in the anticyclonic case (Garreaud et al., 2001). To the east of the Andes, both low- and high-pressure cells are markedly deflected to lower latitudes. Near the east coast of the continent, cyclones usually deepen dramatically (Taljaard, 1972; Sinclair, 1994), in part because of the diabatic effect of the warm waters of the subtropical Atlantic (Seluchi and Saulo, 1998).

Low-Level Effects To describe further the effects of topography on weather systems, the life cycle of low-level low- and high-pressure cells (steered by a trough-ridge wave in the middle troposphere) moving across South America is schematized in figure 3.4. Over the southeast Pacific Ocean, the persistent subtropical anticyclone limits the equatorward extent of the low cell to about 35°S (fig. 3.4a), while the blocking effect of the Andes upon the northwesterly flow (ahead of the surface low) tends to delay the arrival of the cold fronts to the west coast of the continent (Rutllant and Garreaud, 1995). Eventually, the low-pressure cell moves into the southern tip of the continent and the cold front is able to reach the coast, producing rainfall in southern and central Chile and snowfall over the high subtropical Andes (fig. 3.4b).

At the same time, strong westerly winds over the Andes produce lee-side subsidence in western-central Argentina, leading to the formation of a thermal-orographic depression. This later effect, acting in concert with cyclonic vorticity advection aloft, produces the advance of the surface low toward lower latitudes (fig. 3.4b). During the warm

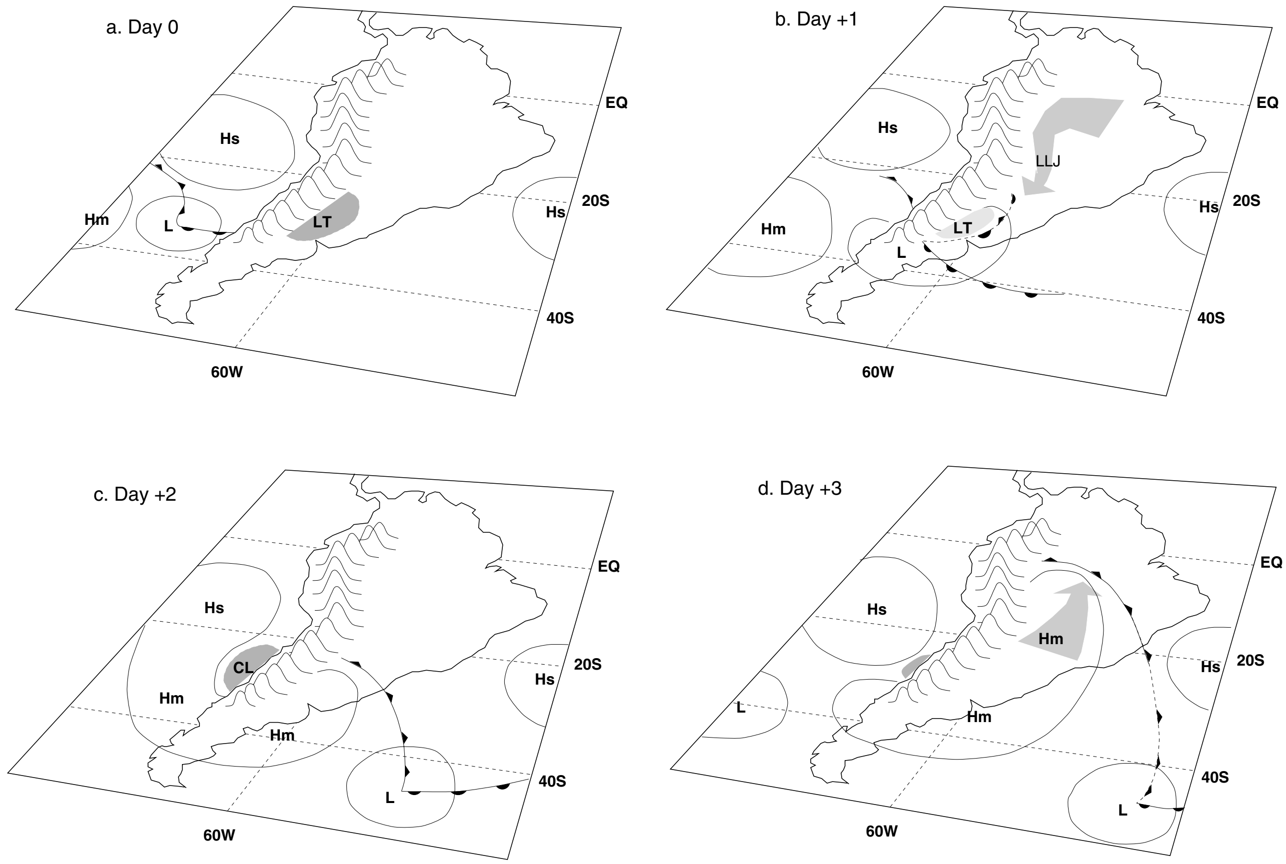

Figure 3.4 Conceptual model of a midlatitude wave moving across South America (for clarity, only surface and low-level features are shown). Solid lines represent isobars at the surface. Recall the clockwise (counter-clockwise) circulation of geostrophic winds around a low (high) pressure cell in the Southern Hemisphere. Hs = subtropical anticyclone; Hm = migratory (cold) anticyclone; L = migratory low pressure cell; LT = lee trough; CL = coastal low. Also shown are surface cold fronts (solid lines with filled triangles), warm fronts (solid lines with filled semicircles), the approximate position of the low-level jet (LLJ, shaded arrow), and the path of the cold air surge (shaded arrow pointing northward). The whole sequence takes about 4 days.

season, the lee-side subsidence deepens the climatological Chaco low, which in turn intensifies the transport of moist, warm air from the Amazon basin toward the subtropical plains, fueling severe storms in the form of prefrontal squall lines or other mesoscale convective complexes (Velasco and Fritsch, 1987; Garreaud and Wallace, 1998; Seluchi and Marengo, 2000). The latent heat release in these storms further deepens the surface low as it moves eastward, thus triggering a positive feedback mechanism (Seluchi and Saulo, 1998). The increasing availability of moist air toward the east coast also contributes to storm intensification. Consistently, explosive cyclogenesis (or cyclone redevelopment) is observed near the east coast of the continent between 25–35°S, especially in the spring and fall, when the synoptic forcing at these latitudes is still strong and the troposphere is unstable (Gan and Rao 1994a;Sinclair, 1994). During the austral winter, thermodynamic conditions over the subtropical plains are less conducive to moist convection but the formation of the lee-trough can, under some conditions, forces severe damaging downslope wind storms along the eastern foothills of the Andes, locally known as *Zonda* events (Norte and Silva, 1995).

To return to the synoptic sequence of figure 3.4, as the surface low moves eastward into the Atlantic, a migratory cold-core anticyclone approaches the west coast of the continent and merges with the subtropical anticyclone over the southeast Pacific (fig. 3.4c). Off the coast of central Chile, the easterly geostrophic winds in the lower troposphere force downslope flow over the Andean slope, so that cool marine air is replaced by warm, continental air. Consequently, the surface pressure drops along the subtropical west coast of the continent, leading to the formation of a coastal low and broad clearing of the stratocumulus clouds over the subtropical Pacific (Garreaud et al., 2001), with significant impacts on regional weather. To the east of the subtropical Andes, the easterly flow along the northern flank of the migratory high is dammed by the mountains, breaking down the geostrophic balance and leading to southerly wind over a band of country about 1,000 km wide beyond the Andean foothills. The cold, dry air surges equatorward between the Andes and the Brazilian plateau, displacing relatively warm, moist air (fig.3.4d). This latter effect results in a hydrostatic rise in surface pressure, explaining the expansion of the surface anticyclone into subtropical and tropical latitudes (Garreaud, 1999a).

Cold surges are a year-round feature of the synoptic climatology of the South American continent (e.g., Kousky and Cavalcanti, 1997; Garreaud, 2000b; Vera and Vigliarolo, 1999; Seluchi and Marengo, 2000), with a near-weekly periodicity but a large range in their intensity and meridional extent. Extreme wintertime episodes (one every few years) produce freezing conditions and severe agricultural damage from central Argentina to southern Bolivia and Brazil (locally known as *friagems* or *geadas*), and have motivated case studies by Hamilton and Tarifa (1978), Fortune and Kousky (1983), and Marengo et al. (1997), among others. Summertime episodes produce less dramatic fluctuations in temperature and pressure, owing to the smaller seasonal temperature gradient between mid- and low latitudes, but they are accompanied by synoptic-scale bands of deep convection at the leading edge of the cool air (Ratisbona, 1976; Kousky, 1979; Garreaud and Wallace, 1998; Liebmann et al., 1999). The banded cloud pattern extends from the eastern slopes of the Andes southeastward into the South Atlantic Ocean, where it intensifies the SACZ. These bands account for up to 40% of the summertime precipitation over subtropical South America (Garreaud and Wallace, 1998) and can reach as far as the northeast coast of Brazil (Kousky, 1979) and across the equator (Parmenter, 1976; Kiladis and Weickmann, 1997).

Cutoff Lows Cutoff lows are isolated cyclonic vortices in the upper troposphere at subtropical and higher latitudes, which develop from preexisting cold troughs (Carlson, 1998). Over South America, cutoff lows are observed over the northeast coast of Brazil and to the west of the subtropical Andes. In the former location, they are a frequent summertime phenomenon (Kousky and Gan, 1981) that dramatically intensifies the climatological trough in this region (fig. 3.2c). Kousky and Gan documented that cutoff lows tend to form near the axis of a SH trough crossing the eastern side of the continent, and they exhibit a direct thermal circulation, with colder air subsiding in their core (inhibiting convection) and warmer air ascending on their periphery (fostering deep convection). Once formed, the vortex may persist for several days, with an irregular horizontal movement, and is associated with excessively dry or wet conditions over northeast Brazil (Kousky and Gan, 1981, Satyamurty et al., 1998).

Cutoff lows to the west of the subtropical Andes also form from a SH trough approaching this region. The segregation of the cold vortex occurs when the zonal flow farther south is very strong (Pizarro and Montecinos, 2000). Once formed, the cutoff low moves rather irregularly along the west side of the Andes, causing strong windstorms and heavy precipitation on the Andean slopes. In contrast with cold fronts that rarely affect latitudes to the north of 30°S, wintertime cutoff lows can produce significant snowfall at higher elevations in northern Chile and Argentina (Pizarro and Montecinos, 2000) and the southern Altiplano (Vuille and Ammann, 1997) a few times a year.

3.2.2 Intraseasonal Variability

Atmospheric fluctuations with periods ranging from 10 to 90 days are generally termed intraseasonal (IS) variability. IS variability in the tropics has been the subject of substantial research since a planetary-scale tropical oscillation with a 40- to 50-day period was discovered in the early 1970s (Madden and Julian, 1971, 1972). It is believed that the Madden-Julian Oscillation (MJO) is primarily forced by anomalies in tropical SST and their feedback in circulation and convection (Madden and Julian, 1994). The MJO-related convection does not directly affect South America, since the associated tropical region of active convection normally moves from the eastern Indian Ocean to the western Pacific and then decays over the eastern Pacific (Salby and Hendon, 1994). In contrast, the MJO-related circulation anomalies at low-latitudes are circumglobal, causing a reversal in the upper level zonal wind over tropical (10°S to 10°N) South America over an ~30-day period. Whether these circulation fluctuations could produce IS variability in the convection over the equatorial Andes and western Amazonia needs to be addressed. IS variability in the subtropics and higher latitudes, although generally less pronounced than the fluctuations associated with individual disturbances, can modulate the regional weather over extended periods of time. IS variability in the extratropics can result from internal nonlinear atmospheric dynamics, or be remotely forced from the tropics by so-called atmospheric teleconnections (see details in Kiladis and Mo, 1998).

Over tropical and subtropical South America, the most notable IS fluctuation is a seesaw of dry and wet conditions with periods ranging between 2 and 3 weeks during the austral summer (Nogués-Paegle and Mo, 1997; Liebmann et al., 1999, Aceituno and Montecinos, 1997). Convection and precipitation over the Altiplano is also organized in rainy episodes of about 1 to 3 weeks, interrupted by similar dry episodes (Aceituno and Montecinos, 1997, Garreaud, 1999b, Lenters and Cook, 1999), and tend to be out-of-phase with convection over the eastern side of the continent (Garreaud, 1999b). The IS variability of the convective rainfall is associated with continental-scale anomalies of the tropospheric circulation, illustrated in figure 3.5 by the 200-hPa height difference and 850-hPa wind difference between positive and negative events (each of them lasting a week or longer) of the rainfall seesaw identified by Nogués-Paegle and Mo (1997). This difference is associated with rainy conditions over the subtropical plains and dry conditions over the SACZ (wet-continent phase of the seesaw). The anticyclonic anomalies at lower-levels enhance the northerly flow and moisture transport to the east of the Andes that in turn feeds convection over the subtropical plains. At upper level, the anticyclonic anomalies intensify and extend southward the region of easterly flow over the Andes associated with the Bolivian High. Easterly flow aloft is typically connected with rainy conditions over the Altiplano, since it fosters the transport of moist air from the Bolivian lowlands to higher elevations (Garreaud, 1999b). Finally, the dry conditions over the SACZ are explained by subsidence downstream of the upper-level anticyclone. Roughly opposite mechanisms act during the dry-continent phase of the seesaw.

It has been proposed that the summertime circulation anomalies over South America (fig. 3.5) are part of large-scale wave train emerging from the South Pacific, referred to as the Pacific South American (PSA) modes. During wintertime, the PSA modes dominate the intraseasonal variability in the SH (Ghil and Mo, 1991; Mo and Higgins, 1997). Mo and Higgins (1997) suggest that tropical convection over the western Pacific serves as a catalyst in the development of standing PSA modes, therefore connecting intraseasonal variability in the remote tropics with intraseasonal variability in subtropical South America.

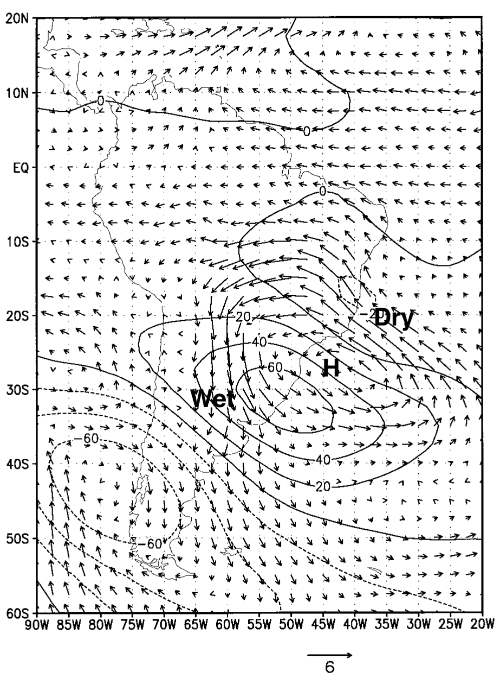

Figure 3.5 200 hPa height difference (contoured every 20 m) and 850 hPa winds (scale in m/s at bottom) difference between the wet-continent and dry-continent phases of the subtropical rainfall seesaw during summer (from Nogués-Paegle and Mo, 1997).

The PSA modes have also been associated with the onset of blocking anticyclones in the south Pacific to the west of the Antarctic Peninsula (Renwick and Revell, 1999), and whose subsequent maintenance arises from a complex interaction between the mean flow and the transient disturbances (Marques and Rao, 1999). The tropospheric-deep anticyclonic anomalies (barotropic structure) tend to split the mid-latitude zonal flow into equatorward and poleward branches. As the blocks in the southeast Pacific remain stationary for 5 to 15 days (Sinclair, 1996; Renwick, 1998), the mid-latitude storm track shifts equatorward, producing stormy conditions in central Chile and dry, cold conditions at the southern tip of the continent (Rutllant and Fuenzalida, 1991).

3.3 Low-Frequency Climatic Variability

Low-frequency climate variability includes changes occurring between consecutive years, usually identified as interannual variability (IA), and slower changes at timescales of decades (interdecadal variability) or longer periods (trends).

Many factors determine interannual climate variability in South America. As elsewhere in the world, those associated with the occurrences of El Niño (EN) and La Niña phenomena in the tropical Pacific, during the extreme phases of the Southern Oscillation (SO), have received much more attention, particularly concerning their impacts on rainfall. The worldwide signatures of ENSO in surface pressure and rainfall were first recognized by Walker and Bliss (1932), and the link between the atmospheric anomalies and tropical Pacific SST anomalies was discovered in the late 1950s and 1960s (e.g. Bjerknes, 1966). Because of its impact and complex dynamics, research literature on ENSO is extensive, and the reader is referred to the volumes of Philander (1990), Diaz and Markgraf (2000), and Glantz et al. (1991) for in-depth treatments of this phenomenon (see also chapter 19).

The sign and strength of the ENSO-related anomalies are geographically and seasonally dependent, rendering a complex picture of the functioning of this phenomenon in the South American region (Aceituno, 1988; Kiladis and Diaz, 1989; Ropelewski and Halpert, 1987, 1989). The negative phase of the SO is typically accompanied by positive SST anomalies in the tropical Pacific, while relatively cold conditions prevail during the positive phase of the SO. When these SST anomalies are relatively intense and last for several months, an episode of El Niño (warm conditions) or La Niña (cold conditions) is defined (Trenberth, 1997).

Studies of ENSO-related rainfall anomalies at a global scale indicate that El Niño episodes are typically associated with below-normal rainfall in the northern part of

South America and anomalously wet conditions in the southeastern portion of the continent, including southern Brazil, Uruguay, southern Paraguay, and northeast Argentina (fig. 3.6; Ropelewski and Halpert, 1987). Opposite rainfall anomalies are typically observed in both regions during La Niña events (Ropelewski and Halpert, 1989). This large picture of the ENSO impacts on rainfall in South America exhibits considerable variation when analyzed at a regional scale.

Hydrological records for the two largest rivers in the northern Andes, the Magdalena and Cauca, show a distinct ENSO signal, indicating a tendency for drought during El Niño episodes and flooding conditions during La Niña events (Aceituno and Garreaud, 1995). The strength of this signal reaches a maximum during the boreal winter (January–February) that coincides with one minimum in the rainfall semi-annual cycle that characterizes this region (Aceituno, 1988; Hastenrath, 1990). Mechanisms involved in this ENSO-related anomaly in the rainfall regime are not well understood. The weakening of the temperature contrast between the continent and adjacent oceans (Pacific and the Caribbean) and the enhanced convection over the eastern tropical Pacific during an El Niño episode are two factors favoring a weakening of convection over the Colombian Andes.

Flood conditions along the semi-arid coastal areas in southern Ecuador and northern Peru during El Niño episodes are one of the trademarks of the climatic impacts of this phenomenon in South America (see Chapter 19). In fact, many decades before coherent global-scale climate anomalies were linked to ENSO, the damaging floods during episodes of anomalously warm waters along the coast of northern Peru had been well documented (e.g., Murphy, 1926). As in most regions having a significant ENSO signal on climate variability, rainfall anomalies here are phase-locked with the annual rainfall cycle. Thus, flood conditions during El Niño events develop from around December to May, and there is evidence that strong convection-producing rainfall is triggered by anomalously high values of SST in the adjacent ocean (Horel and Cornejo-Garrido, 1986). Although enhanced convection and rainfall are confined to lowland areas near the coast, the impact on river discharges is extremely large. As an example, at the peak of the major 1982–1983 El Niño episode, in May 1983 when SST surpassed 28.0°C along the coast of northern Perú, the discharge of the Piura River neared 1,200 m^3/s, well above its average flow of about 40 m^3/s for that month!

Over the central Andes, especially along the western side of the Altiplano, a relatively weak tendency for drier-than-average conditions during the wet season (December–March), when positive SST anomalies prevail in the tropical Pacific, has been documented in several studies (Francou and Pizarro, 1985; Ronchail, 1995; Vuille, 1999). This anomalous behavior in the rainfall regime produces a significant mark on hydrological and glaciological records. Specifically, El Niño episodes are associated with a relatively low seasonal increment in the level of Lake Titicaca (Kessler, 1974; Aceituno and Garreaud, 1995)) and below-average snow accumulation on glaciers (Thompson et al., 1984; Wagnon et al., 2001). Negative rainfall anomalies during El Niño are consistent with stronger-than-average subtropical westerlies over the Altiplano, conditions that inhibit the advection of moisture from the warm and humid environment of the Bolivian lowlands (). Opposite upper-level circulation anomalies tend to occur during wet seasons coinciding with La Niña episodes, thus enhancing the moisture transport toward the Altiplano and favoring wetter-than-average conditions.

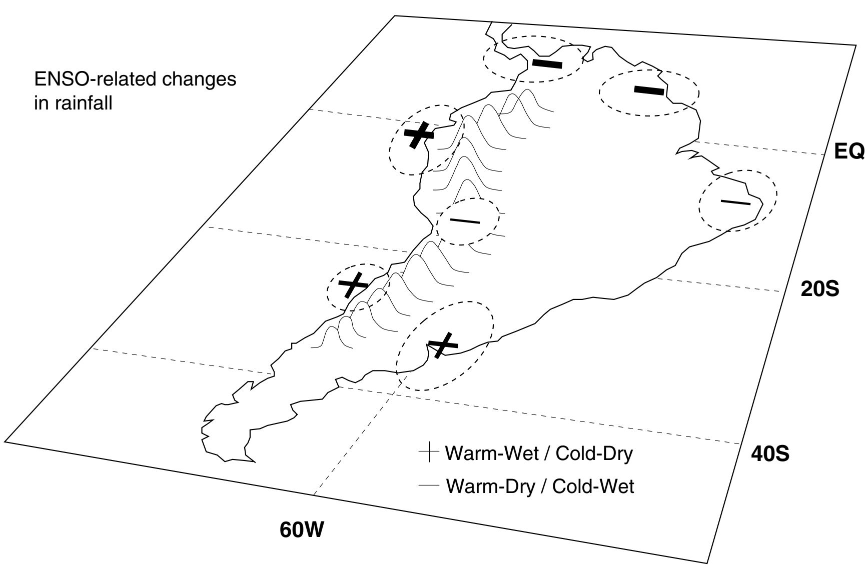

Figure 3.6 Main areas with ENSO-related changes in rainfall. The affected regions are approximately outlined by dashed lines. The correlation between rainfall anomalies and tropical Pacific SST (an index of ENSO) is indicated by plus and minus signs, the thickness of which indicates the relative strength of the correlation. The strongest rainfall anomalies tend to occur during the corres ponding climatological wet season.

Long recognized is the tendency for drought to occur in semiarid northeast Brazil (the Brazilian Nordeste) when El Niño conditions prevail in the tropical Pacific (e.g., Caviedes, 1973). Nevertheless, the interannual rainfall variability in this part of the continent has stronger links to anomalous SST, surface wind, and convection patterns in the tropical Atlantic, conditions that are partially modulated by ENSO (Hastenrath and Heller, 1977; Moura and Shukla, 1981). A dipole of SST anomalies over the Atlantic on both sides of the equator sometime persists for several months. Warm SST anomalies to the north of the equator lead to enhanced convection in the ITCZ and stronger-than-normal subsidence and drought over the Nordeste (Moura and Shukla, 1981). When SST warm anomalies occur to the south of the equator, the ITCZ encompasses the Nordeste, causing wetter than normal conditions there.

Changes in the global atmospheric circulation induced by anomalies in the ocean-atmosphere system in the tropical Pacific are at the origin of many ENSO-related climate anomalies in subtropical and extratropical areas around the globe (that is, teleconnection patterns). In South America, these signals are significant along the subtropical western border (central Chile) and over the southeast portion of the continent. Regarding the links between SST anomalies in the tropical Pacific and rainfall, a warm-wet / cold-dry relationship over central Chile and the subtropical Andes during the wet season (May–September) has been documented in several studies (Quinn and Neal, 1983; Kiladis and Diaz, 1989; Aceituno and Garreaud, 1995). A detailed analysis of this ENSO signal revealed that the tendency for positive (negative) rainfall anomalies during El Niño (La Niña) is significant in the 33°S to 36°S latitudinal band during the austral winter, while from 36°S to 39°S the same signal is best defined during the spring (Montecinos et al., 2000). The tendency to above average wintertime rainfall during El Niño years is consistent with a relatively higher frequency of blocking anticyclones to the west of the Antarctic Peninsula, and the subsequent northward displacement of the South Pacific storm track (Rutllant and Fuenzalida, 1991).

Over southeastern South America, anomalously wet conditions typically occur during El Niño that generate extensive flooding in the lowlands of southern Brazil, southern Paraguay, Uruguay, and northeast Argentina. Several studies have described this ENSO-related signal based on the analysis or rainfall and streamflow records (Kousky et al., 1984; Aceituno, 1988; Pisciottano et al., 1994; Diaz et al., 1998; Grimm et al., 1998). This relationship between ENSO and rainfall has been linked to the intensification of the subtropical jet and its associated baroclinic activity (Kousky et al., 1984; Lenters and Cook, 1999). Its strength is greatest during the austral spring and early summer (Montecinos et al., 2000).

It has been recognized that central Pacific SST anomalies during warm and cold episodes are accompanied by temperature anomalies of the same sign in the tropical troposphere throughout the globe. Over South America, there is a clear tendency for above (below) normal air temperature during warm (cold) ENSO years, from the northern margins of the continent south to about 30°S (Aceituno, 1988, 1989). The opposite relationship (that is, cold air anomalies during El Niño years) is observed in midlatitudes year-round and along the subtropics during the early summer, probably because ENSO-related increased precipitation over these regions is also associated with a reduction of solar radiation (Aceituno, 1988).

One must keep in mind that the relationships between ENSO and regional rainfall and temperature, as described above, are typically obtained from data records during the last 30 to -40 years. The strength of these relationships might vary significantly when viewed on longer timescales (Aceituno and Montecinos, 1993). It is also important to remember that ENSO is only one of the significant factors modulating interannual climatic variability in South America. In fact, many studies have demonstrated the significant influence that changes in the tropical Atlantic ocean-atmospheric system have on rainfall variability over many areas of tropical South America (Hastenrath and Heller, 1977; Marengo, 1992; Nobre and Shukla, 1996; Diaz et al., 1998)

Recent work has focused on interdecadal variability of the ocean-atmosphere system that may explain slow or abrupt changes in climate. The broadly known "regime shift" of 1976 appears to be an outstanding example (e.g., Graham, 1994). Yet our capacity to identify, describe, and explain this interdecadal climate variability is hampered by the relatively short length of the instrumental records relative to the timescale to be addressed (Garreaud and Battisti, 1999). At even longer timescales, slow changes in the climate are present as trends in almost all climatic records. Slowly evolving boundary conditions of the atmosphere (mostly SST) seem to be the most important factors influencing this type of variability. In subtropical South America, a marked contrast is apparent in the long-term evolution of rainfall on both sides of the continent. On the western margin (central Chile), a negative trend characterized most of the rainfall records during the twentieth century (Aceituno et al., 1992), while on the eastern side a remarkable upward trend has been observed on rainfall and streamflow records, especially after 1950 (Krepper et al., 1989; Castañeda and Barros, 1994; Minetti and Vargas, 1997; Robertson and Mechoso, 1998).

References

Abreu, M., and P. Bannon, 1993. Dynamics of the South American Coastal Desert. *Journal of Atmospheric Sciences*, 50, 2952–2964.

Aceituno, P., 1988. On the functioning of the Southern Oscillation in the South American sector. Part I: Surface climate. *Monthly Weather Review*, 116, 505–524.

Aceituno, P., 1989. On the functioning of the Southern Oscillation in the South American sector. Part II: Upper-air circulation. *Journal of Climate*, 21, 341–355.
Aceituno, P., H. Fuenzalida, and B. Rosenbluth, 1992. Climate along the extratropical west coast of South America. In: H.A. Mooney, B. Kronberg, and E.R. Fuentes (Editors), *Earth system responses to global change*. Academic Press, New York, 61–96.
Aceituno, P., and R.D. Garreaud, 1995. The impact of the ENSO phenomenon in the pluviometric regime over the Andes. *Revista Chilena de Ingeniería Hidraulica,* 2, 33–43.
Aceituno, P., and A. Montecinos, 1993. Estabilidad de la relación entre la Oscilación del Sur y la precipitación en América del Sur. *Bulletin Institut Français Etudes Andines*, 22, 53–64.
Aceituno, P., and A. Montecinos, 1997. Patterns of convective cloudiness in South America during austral summer from OLR pentads. In: Preprints, Fifth International Conference on Southern Hemisphere Meteorology and Oceanography, Pretoria, South Africa. *American Meteorological Society*, Boston, 328–329.
Berbery, E.H., and E. Collini, 2000. Springtime precipitation and water-vapor flux convergence over southeastern South America. *Monthly Weather Review*, 128, 1328–1346.
Berbery, E.H., and C.S. Vera, 1996. Characteristics of the Southern Hemisphere winter storm track with filtered and unfiltered data. *Journal of Atmospheric Sciences,* 53, 468–481.
Bjerknes, J., 1966. A possible response of the atmospheric Hadley circulation to equatorial anomalies of ocean temperature. *Tellus*, 18, 820–829.
Carlson, T.N., 1998. *Mid-latitude weather systems*. American Meteorological Society. Boston.
Castañeda, M.E., and V.R. Barros, 1994. Long-term trends in rainfall along southern South America eastward from the Andes. *Meteorológica*, 19, 23–32.
Caviedes, C.N., 1973. Secas and El Niño: Two simultaneous climatological hazards in South America. *Proceedings of the Association of American Geographers*, 5, 44–49.
Cohen J., M. Silva Dias, and C. Nobre, 1995. Environmental conditions associated with Amazonian squall lines: A case study. *Monthly Weather Review*, 123, 3163–3174.
Diaz, H.F., and V. Markgraf, 1992. *El Niño*. Cambridge University Press, Cambridge.
Diaz, A.F., C.D. Studzinski, and C.R. Mechoso, 1998. Relationships between precipitation anomalies in Uruguay and southern Brazil and sea surface temperature in the Pacific and Atlantic Oceans. *Journal of Climate*, 11, 251–271.
Figueroa, S.N., P. Satyamurty, and P.L. Silva Dias, 1995. Simulation of the summer circulation over the South American region with an Eta coordinate model. *Journal of Atmospheric Sciences*, 52, 1573–1584.
Fortune, M.A., and V.E. Kousky, 1983. Two severe freezes in Brazil: Precursors and synoptic evolution. *Monthly Weather Review*, 111, 181–196.
Francou, B., and L. Pizarro, 1985. El fenómeno de El Niño y las sequias en los Andes centrales (Perú y Bolivia). *Bulletin Institut Français Etudes Andines*, 14, 1–18.
Fu, R., B. Zhu, and R.E. Dickinson, 1999. How do atmosphere and land surface influence seasonal changes of convection in the tropical Amazon? *Journal of Climate*, 12, 1306–1321.
Gan, M.A., and V. Rao, 1994a. Surface cyclogenesis over South America. *Monthly Weather Review*, 119, 1923–1302.
Gan, M.A., and V. Rao, 1994b. The influence of the Andes cordillera on transient disturbances. *Monthly Weather Review*, 122, 1141–1157.
Gandu, A.W., and P.L. Silva Dias, 1998. Impact of tropical heat sources on South American tropospheric circulation and subsidence. *Journal of Geophysical Research*, 103, 6001–6015.
Garreaud, R.D., 1999a. Cold air incursions over subtropical and tropical South America. A numerical case study. *Monthly Weather Review,* 127, 2823–2853.
Garreaud, R.D., 1999b. A multi-scale analysis of the summertime precipitation over the central Andes. *Monthly Weather Review*, 127, 901–921.
Garreaud, R.D., 2000a. Intraseasonal variability of moisture and rainfall over the South American Altiplano. *Monthly Weather Review*, 128, 3379–3346.
Garreaud, R.D., 2000b. Cold air incursions over Subtropical South America: Mean structure and dynamics. *Monthly Weather Review*, 128, 2544–2559.
Garreaud, R.D., and D.S. Battisti, 1999. Interannual (ENSO) and interdecadal (ENSO-like) variability in the Southern Hemisphere tropospheric circulation. *Journal of Climate*, 12, 2113–2123.
Garreaud, R.D, and J.M. Wallace, 1997. The diurnal march of convective cloudiness over the Americas. *Monthly Weather Review*, 125, 3157–3171.
Garreaud, R.D., and J.M. Wallace, 1998. Summertime incursions of midlatitude air into tropical and subtropical South America. *Monthly Weather Review*, 126, 2713–2733.
Garreaud, R.D., J. Rutllant, and H. Fuenzalida, 2002. Coastal lows in the subtropical western coast of South America: Mean structure and evolution. *Monthly Weather Review*, 130, 75–88 .
Garreaud, R.D., J. Rutllant, J. Quintana, J. Carrasco, and P. Minnis, 2001. CIMAR-5: A snapshot of the lower troposphere over the subtropical Southeastern Pacific. *Bulletin of the American Meteorological Society*, 82, 2193–2207.
Ghil, M., and K.C. Mo, 1991. Intraseasonal oscillations in the global atmosphere. Part II: Southern Hemisphere. *Journal of Atmospheric Sciences*, 48, 780–790.
Glantz, M., R. Katz, and N. Nicholls (Editors), 1991. *Teleconnections linking worldwide climate anomalies*. Cambridge University Press. Cambridge.
Graham, N.E., 1994. Decadal-scale climate variability in the 1970s and 1980s: Observations and model results. *Climate Dynamics*, 10, 135–162.
Grimm, A.M., S.E. Ferraz, and J. Gomes, 1998. Precipitation anomalies in southern Brasil associated with El Niño and La Niña events. *Journal of Climate*, 11, 2863–2880.
Gutmann, G., and W.S., Schwerdtfeger, 1965. The role of the latent and sensible heat for the development of a high pressure system over the subtropical Andes in the summer. *Meteorologische Rundschau*, 18, 1–17.
Hamilton, M.G., and J.R. Tarifa, 1978. Synoptic aspects of a polar outbreak leading to frost in tropical Brazil, July 1972. *Monthly Weather Review*, 106, 1545–1556.
Hartmann, D.L., M.E. Ockert-Bell, and M.L. Michelsen, 1992. The effect of cloud type on Earth´s energy balance: Global analysis. *Journal of Climate*, 5, 1281–1304.

Hastenrath, S., 1982. *Climate dynamics of the tropics*. 2nd ed., Kluwer, New York.
Hastenrath, S., 1990. Diagnostics and prediction of anomalous river discharge in northern South America. *Journal of Climate*, 3, 1080–1096.
Hastenrath, S., and L. Heller, 1977. Dynamic of climate hazards in Northeast Brazil. *Quarterly Journal of the Royal Meteorological Society*, 103, 77–92.
Hobbs, J.E., J.A., Lindeasay, and H.A. Bridgman (Editors), 1998. *Climate of the southern continents: Present, past and future*. John Wiley. Chichester.
Holton, J.R., 1992. *An introduction to dynamic meteorology*. 3rd ed., Academic Press. New York.
Horel, J., and A.G. Cornejo-Garrido, 1986. Convection along the coast of Northern Peru during 1983: Spatial and temporal variations in cloud and rainfall. *Monthly Weather Review*, 114, 2091–2105.
Horel, J., A. Hahmann, and J. Geisler, 1989. An investigation of the annual cycle of the convective activity over the tropical Americas. *Journal of Climate*, 2, 1388–1403.
Kalnay, E., and others, 1996. The NCEP/NCAR 40–years reanalysis project. *Bulletin of the American Meteorological Society*, 77, 437–472.
Kessler, A., 1974. Atmospheric circulation anomalies and level fluctuations of Lake Titicaca. *Bonner Meteorologisch Abh*. 17, 361–372.
Kiladis, G.N., and H. Diaz, 1989. Global climatic anomalies associated with extremes in the Southern Oscillation. *Journal of Climate*, 2, 1069–1090.
Kiladis, G.N., and K.M. Weickmann, 1997. Horizontal structure and seasonality of large-scale circulations associated with submonthly tropical convection. *Monthly Weather Review*, 125, 1997–2013.
Kiladis, G.N., and K.C. Mo, 1998. Interannual and intraseasonal variability in the Southern Hemisphere. In: D. Karoly and D. Vincent (Editors), *Meteorology of the Southern Hemisphere. Meteorological Monographs,* No. 49. American Meteorological Society. Boston, 307–336.
Klein, S.A., and D.L. Hartmann, 1993. The seasonal cycle of low stratiform clouds. *Journal of Climate*, 6, 1587–1606.
Kodoma, Y., 1992. Large-scale common features of subtropical precipitation zones (the Baiu frontal zone, the SPCZ and the SACZ). Part I: Characteristic of subtropical frontal zones. *Journal of the Meteorological Society of Japan*, 70, 813–836.
Kousky, V.E., 1979. Frontal influences on northeast Brazil. *Monthly Weather Review*, 107, 1140–1153.
Kousky, V.E., and I. Cavalcanti, 1997. The principal modes of high-frequency variability over the South American region. In: Preprints Fifth International Conference on Southern Hemisphere Meteorology & Oceanography, Pretoria, South Africa. American Meteorological Society, Boston, 7B2–7B3.
Kousky, V.E., and J. Ferreira, 1981. Frontal influences on northeast Brazil: their spatial distributions, origins and effects. *Monthly Weather Review*, 109, 1999–2008.
Kousky, V.E., and M.A. Gan, 1981. Upper tropospheric cyclonic vortices in the tropical South Atlantic. *Tellus*, 33, 538–551.
Kousky, V.E., M.T. Kagano, and I.F. Cavalcanti, 1984. A review of the Southern Oscillation: Oceanic-atmospheric circulation changes and related rainfall anomalies. *Tellus*, 36a, 490–504.
Krepper, C.M., B. Scian, and J. Pierini, 1989. Time and space variability of rainfall in central-east Argentina. *Journal of Climate*, 2, 39–47.
Legates, D.R., and C. Willmott, 1990. Mean seasonal and spatial variability in gauge-corrected global precipitation. *International Journal of Climatology*, 10, 111–127.
Lenters, J.D., and K.H. Cook, 1995. Simulation and diagnosis of the regional summertime precipitation climatology of South America. *Journal of Climate*, 8, 2298–3005.
Lenters, J.D., and K.H. Cook, 1997. On the origin of the Bolivian High and related circulation features of the South American climate. *Journal of Atmospheric Sciences*, 54, 656–677.
Lenters, J.D., and K.H. Cook, 1999. Summertime precipitation variability over South America: Role of the large-scale circulation. *Monthly Weather Review*, 127, 409–431.
Liebmann, B., G. Kiladis, J. Marengo, T. Ambrizzi, and J.D. Glick, 1999. Submonthly convective variability over South America and the South Atlantic Convergence Zone. *Journal of Climate*, 11, 2898–2909.
Madden, R., and P. Julian, 1971. Detection of a 40–50 day oscillation in the zonal wind. Journal of Atmospheric Sciences, 28, 702–708.
Madden, R., and P. Julian, 1972. Description of global-scale circulation cells in the Tropics with a 40–50–day period. *Journal of Atmospheric Sciences*, 29, 1109–1123.
Madden, R., and P. Julian, 1994. A review of the intraseasonal oscillation in the Tropics. *Monthly Weather Review*, 122, 814–837.
Marengo, J., 1992. Interannual variability of surface climate in the Amazon basin. *International Journal of Climatology*, 12, 853–863.
Marengo, J., A. Cornejo, P. Satymurty, C. Nobre, and W. Sea, 1997. Cold surges in tropical and extratropical South America: The strong event in June 1994. *Monthly Weather Review*, 125, 2759–2786.
Marques, R., and V.B. Rao, 1999. A diagnosis of a long-lasting blocking event over the southeast Pacific Ocean. *Monthly Weather Review*, 127, 1761–1776.
Meisner, B., and P. Arkin, 1987. Spatial and annual variations in the diurnal cycle of the large-scale tropical convective cloudiness and precipitation. *Monthly Weather Review*, 115, 2009–2032.
Minetti, J.L., and W.M. Vargas, 1997. Trends and jumps in the annual precipitation in South America south of the 15°S. *Atmósfera*, 11, 205–221.
Mitchell, T.P., and J.M. Wallace, 1992. The annual cycle in the equatorial convection and sea surface temperature. *Journal of Climate*, 5, 1140–1156.
Mo, K.C., and R.W. Higgins, 1997. The Pacific-South American mode and tropical convection during the Southern Hemisphere winter. *Monthly Weather Review*, 126, 1581–1596.
Montecinos, A., A. Diaz, and P. Aceituno, 2000. Seasonal diagnostic and predictability of rainfall in subtropical South America based on Tropical Pacific SST. *Journal of Climate*, 13, 746–758.
Moura, A.D., and J. Shukla, 1981. On the dynamics of droughts in northeast Brazil: Observations, theory and numerical experiments with a general circulation model. *Journal of Atmospheric Sciences*, 38, 2653–2675.
Murphy, R.C., 1926. Oceanic and climatic phenomena along the west coast of South America during 1925. *Geographical Review*, 16, 26–64.

Negri, A., R. Adler, E. Nelkin, and G. Huffman, 1994. Regional rainfall climatologies derived from special sensor microwave imager (SSM/I) data. *Bulletin of the American Meteorological Society*, 75, 1165–1182.

Nigam, S., 1997. The annual warm to cold phase transition in the eastern equatorial Pacific: Diagnosis of the role of stratus cloud-top cooling. *Journal of Climate,* 10, 2447–2467.

Nobre, P., and J. Shukla, 1996. Variations of sea-surface temperature, wind stress and rainfall over the tropical Atlantic and South America. *Journal of Climate*, 9, 2464–2479.

Nogués-Paegle, J., and K.C. Mo, 1997. Alternating wet and dry conditions over South America during summer. *Monthly Weather Review*, 125, 279–291.

Norte, F., and M. Silva, 1995. Predicting severe versus moderate Zonda wind in Argentina. In: Preprints of the 14th Conference on Weather Analysis and Forecasting. American Meteorological Society. Boston, 128–129.

Parmenter, F.C., 1976. A Southern Hemisphere cold front passage at the equator. *Bulletin of the American Meteorological Society*, 57, 1435–1440.

Philander, S.G., 1990. *El Niño, La Niña, and the Southern Oscillation*. Academic Press. New York.

Physick, W.L., 1981. Winter depression tracks and climatological jet streams in the Southern Hemisphere during the FGGE year. *Quarterly Journal of the Royal Meteorological Society*, 107, 883–898.

Pisciottano, G., A. Diaz, G. Cazes, and C.R. Mechoso, 1994. El Niño-Southern Oscillation impact on rainfall in Uruguay. *Journal of Climate*, 7, 1286–1302.

Pizarro, J., and A. Montecinos, 2000. Cutoff cyclones off the subtropical coast of Chile. In: Proceedings of the 6th International Conference on Southern Hemisphere Meteorology and Oceanography. Santiago, Chile, 2000. American Meteorological Society. Boston, 278–279.

Quinn, W.H., and V.T. Neal, 1983. Long-term variations in the Southern Oscillation, El Nino, and the Chilean subtropical rainfall. *Fishery Bulletin*, 81, 1258–1288.

Ratisbona, C. R., 1976. The climate of Brazil. In: W. Schwerdtfeger and H.E. Landsberg (Editors), *Climate of Central and South America*. World Survey of Climatology, 12, Elsevier. New York, 219–293.

Renwick, J.A., 1998. ENSO-related variability in the frequency of South Pacific blocking. *Monthly Weather Review*, 126, 3117–3123.

Renwick, J.A., and M. Revell, 1999. Blocking over the South Pacific and Rossby wave propagation. *Monthly Weather Review*, 127, 2233–2247.

Robertson, A.W., and C.R. Mechoso, 1998. Interannual and decadal cycles in river flows of southeastern South America. *Journal of Climate*, 11, 2570–2581.

Rodwell M.J., and B.J. Hoskins, 1996. Monsoons and the dynamics of deserts. *Quarterly Journal of the Royal Meteorological Society*, 122, 1385–1404.

Ronchail, J., 1995. Variabilidad interanual de las precipitaciones en Bolivia. *Bulletin Institute Français Etudes Andines*, 24, 369–378.

Ropelewski, C.F., and M.S. Halpert, 1987. Global and regional-scale precipitation patterns associated with the El Niño/Southern Oscillation. *Monthly Weather Review*, 115, 1606–1626.

Ropelewski, C.F., and M.S. Halpert, 1989. Precipitation patterns associated with the high index phase of the Southern Oscillation. *Journal of Climate*, 2, 1606–1626.

Rutllant, J., and H. Fuenzalida, 1991. Synoptic aspects of the central Chile rainfall variability associated with the Southern Oscillation. *International Journal of Climatology*, 11, 63–76.

Rutllant, J., and R. Garreaud, 1995. Meteorological air pollution potential for Santiago, Chile: Towards an objective episode forecasting. *Environmental Monitoring and Assessment*, 34, 223–244.

Rutllant, J., H. Fuenzalida, P. Aceituno, A. Montecinos, R. Sanchez, H. Salinas, J. Inzunsa, and R. Zuleta, 2000. Coastal climate dynamics of the Antofagasta region (Chile, 23°S): The 1997–1998 DICLIMA Experiment. In: Proceedings of the 6th International Conference on Southern Hemisphere Meteorology and Oceanography. Santiago, Chile, 2000. American Meteorological Society, Boston, 268–269.

Salby, M. L., and H.H. Hendon, 1994. Intraseasonal behavior of clouds, temperature, and motion in the tropics. *Journal of Atmospheric Sciences*, 51, 2207–2224.

Satyamurty, P., C. Nobre, and P.L. Silva Dias, 1998. South America. In: D. Karoly and D. Vincent (Editors), *Meteorology of the Southern Hemisphere*. Meteorological Monographs No. 49. American Meteorological Society. Boston, 119–140.

Saulo, C., M. Nicolini, and S. Chou, 2000. Model characterization of the South American low-level flow during the 1997–1998 spring-summer season. *Climate Dynamics*, 16, 867–881.

Schwerdtfeger, W.C., 1961. Stromings und Temperatufeld der freien Atmosphare uber den Andes. *Meteorologische Rundshau*, 14, 1–6.

Schwerdtfeger, W., and L. Landsberg (Editors), 1976. *Climate of Central and South America*. Elsevier, New York.

Seluchi, M., and J. Marengo, 2000. Tropical-midlatitude exchange of air masses during summer and winter in South America: Climatic aspects and examples of intense events. *International Journal of Climatology*, 20, 1167–1190.

Seluchi, M., and A.C. Saulo, 1998. Possible mechanisms yielding an explosive coastal cyclogenesis over South America: Experiments using a limited area model. *Australian Meteorology Magazine*, 47, 309–320.

Seluchi, M., Y.V. Serafini, and H. Le Treut, 1998. The impact of the Andes on transient atmospheric systems: A comparison between observations and GCM results. *Monthly Weather Review*, 126, 895–912.

Sinclair, M. R., 1994. An objective cyclone climatology for the Southern Hemisphere. *Monthly Weather Review*, 123, 2239–2256.

Sinclair, M. R., 1996. A climatology of anticyclones and blocking for the Southern Hemisphere. *Monthly Weather Review*, 124, 254–263.

Spencer, R. W., 1993. Global oceanic precipitation from the MSU during 1979–91 and comparisons to other climatologies. *Journal of Climate*, 6, 1301–1326.

Taljaard, J.J., 1972. Synoptic meteorology of the Southern Hemisphere. In: *Meteorology of the Southern Hemisphere*. Meteorological Monographs, No. 35, American. Meteorological Society, 139–213.

Thompson, L.G., E. Mosley-Thompson, and B. Morales-Arnao, 1984. El Niño Southern Oscillation as recorded in the stratigraphy of the tropical Quelccaya ice cap, Peru. *Science*, 226, 50–52.

Trenberth, K. E., 1991. Storm tracks in the Southern Hemisphere. *Journal of Atmospheric Sciences*, 48, 2159–2178.

Trenberth, K.E., 1997. The definition of El Niño. *Bulletin of the American Meteorological Society*, 78, 2771–2777.

Velasco, I., and J.M. Fritsch, 1987. Mesoscale convective complexes in the Americas. *Journal of Geophysical Research*, 92, 9591–9613.

Vera, C.S., and P.K. Vigliarolo, 1999. A diagnostic study of cold-air outbreaks over South America. *Monthly Weather Review*, 128, 3–24.

Vigliarolo, P.K., C. Vera, and S. Diaz., 2000. Southern Hemisphere winter ozone fluctuations. *Quarterly Journal of the Royal Meteorological Society*, 61, 1–20.

Vincent, D.G., 1998. Pacific Ocean. Meteorology of the Southern Hemisphere. In: D. Karoly and D. Vincent (Editors), *Meteorology of the Southern Hemisphere*. Meteorological Monographs, No. 49. American Meteorological Society. Boston, 101–118.

Virji, H., 1981. A preliminary study of summertime tropospheric circulation patterns over South America estimated from cloud winds. *Monthly Weather Review*, 109, 599–610.

Vuille, M., 1999. Atmospheric circulation over the Bolivian Altiplano during dry and wet periods and extreme phases of the Southern Oscillation. *International Journal of Climatology*, 19, 1579–1600.

Vuille, M., and C. Ammann, 1997. Regional snowfall patterns in the high arid Andes. *Climatic Change*, 36, 413–423.

Wallace, J.M., and P. Hobbs, 1977. *Atmospheric science: An introductory survey*. Academic Press, San Diego.

Walker, G.T., and E.W. Bliss, 1932. World Weather V. *Memoire of the Royal Meteorological Society*, 4, 53–84.

Wagnon P., P. Ribstein, B. Francou, and J.M. Sicart, 2001. Anomalous heat and mass budget on the Zongo glacier during the 1997–98 El Niño year. *Journal of Glaciology*, 156, 21–28.

Zhou, J., and K.M. Lau, 1998. Does a monsoon climate exist over South America? *Journal of Climate*, 11, 1020–1040.